Coupling of localized moments and itinerant electrons in $EuFe_2As_2$ single crystals studied by Electron Spin Resonance

E. Dengler,[1] J. Deisenhofer,[1,*] H.-A. Krug von Nidda,[1] Seunghyun Khim,[2]
J. S. Kim,[3] Kee Hoon Kim,[2] F. Casper,[4] C. Felser,[4] and A. Loidl[1]

[1] *Experimentalphysik V, Center for Electronic Correlations and Magnetism, Institute for Physics, Augsburg University, D-86135 Augsburg, Germany*
[2] *FPRD, Department of Physics and Astronomy, Seoul National University, Seoul 151-742, Korea*
[3] *Departement of Physics, Pohang University of Science and Technology, Pohang 790-784, Korea*
[4] *Institute for Inorganic and Analytic Chemistry, Johannes Gutenberg-Universität, D-55099 Mainz, Germany*

(Dated: September 10, 2009)

Electron spin resonance measurements in $EuFe_2As_2$ single crystals revealed an absorption spectrum of a single resonance with Dysonian lineshape. Above the spin-density wave transition at T_{SDW} = 190 K the spectra are isotropic and the spin relaxation is strongly coupled to the CEs resulting in a Korringa-like increase of the linewidth. Below T_{SDW}, a distinct anisotropy develops and the relaxation behavior of the Eu spins changes drastically into one with characteristic properties of a magnetic insulating system, where dipolar and crystal-field interactions dominate. This indicates a spatial confinement of the CEs to the FeAs layers in the SDW state.

PACS numbers: 76.30.-v,75.30.Fv,75.20.Hr,71.70.Ch

The discovery of superconductivity in Fe-based pnictides and chalcogenides has released an avalanche of scientific studies in condensed-matter physics and chemistry. Three main material classes are currently spurring the field: the RFeAsO compounds with R=La-Gd (1111-systems) [1, 2], the ternary AFe$_2$As$_2$ class with A=Ba,Sr,Ca,Eu (122-systems) [3, 4], and the binary chalcogenide systems such as FeSe [5, 6, 7]. The parent compounds of the 1111 and 122 systems exhibit a spin density wave (SDW) anomaly which is accompanied by a structural distortion [8, 9, 10]. Upon doping the divalent A-site ions in the 122 compounds by monovalent ions like K the SDW anomaly becomes suppressed and a superconducting ground state appears.

Here we focus on $EuFe_2As_2$ which exhibits a SDW anomaly at T_{SDW} = 190 K [11, 12, 13]. The Eu^{2+} ions with spin $S = 7/2$ order antiferromagnetically at T_N = 19 K [12, 13, 23]. The system reportedly becomes superconducting upon substituting Eu by K [4], As by P [14], or applying external pressure of about 26 kbar [15, 16]. In contrast to the other 122 systems, where the substitution of Fe by Co also leads to superconductivity [17, 18], the Eu compounds exhibit the onset of a superconducting transition but seem to be hindered to reach zero resistivity [19]. It has been suggested that there is a strong coupling between the localized Eu spins and the conduction electrons (CEs) from the two-dimensional (2D) FeAs layers as evidenced by magnetization and magnetoresistance measurements in the parent compound [20].

To elucidate this coupling we investigated single crystalline $EuFe_2As_2$ by electron spin resonance (ESR) spectroscopy. ESR has been shown to be a highly sensitive tool to study the spin fluctuations and magnetic interactions in cuprate superconductors and their parent compounds (see e.g. Ref. 22 and references therein). Our results show that above T_{SDW} the relaxation time of the Eu spins is dominated by the interaction with the CEs, while the Eu system shows a relaxation behavior reminiscent of a magnetic insulator below T_{SDW}.

Polycrystalline $EuFe_2As_2$ was prepared following the procedure described in [21] and characterized by X-ray powder diffraction using Mo-Kα radiation (λ= 0.7093165 nm; Bruker, AXS D8). High-quality $EuFe_2As_2$ single crystals were grown using flux technique with starting composition of Eu:Fe:As:Sn = 1:2:2:19, where Sn was removed by centrifugation after crystal growth. The good quality of the single crystals was confirmed by Laue x-ray diffraction as well as scanning electron microscopy equipped with energy dispersive x-ray analysis. The in-plane resistivity was measured using a standard 4-probe method. For magnetization measurements we used a SQUID magnetometer MPMS5 (Quantum Design). ESR measurements were performed in a Bruker ELEXSYS E500 CW-spectrometer at X-band frequencies ($\nu \approx 9.36$ GHz) equipped with a continuous He gas-flow cryostat in the temperature region $4.2 < T < 300$ K. ESR detects the power P absorbed by the sample from the transverse magnetic microwave field as a function of the static magnetic field H. The signal-to-noise ratio of the spectra is improved by recording the derivative dP/dH using lock-in technique with field modulation.

Figure 1 shows ESR spectra of $EuFe_2As_2$ for different temperatures and orientations of the single crystal. In all cases one observes a single exchange-narrowed resonance line which is well described by a Dyson shape [24]

$$P(H) \propto \frac{\Delta H + \alpha(H - H_{res})}{(H - H_{res})^2 + \Delta H^2}, \qquad (1)$$

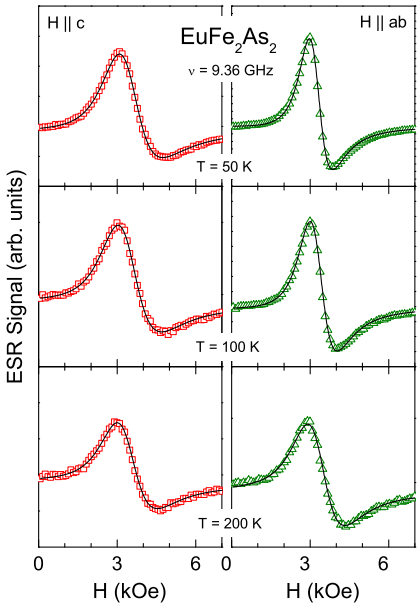

FIG. 1: (Color online) ESR spectra of an $EuFe_2As_2$ single crystal taken at different temperatures for the magnetic field applied parallel (left) and perpendicular (right) to the c axis.

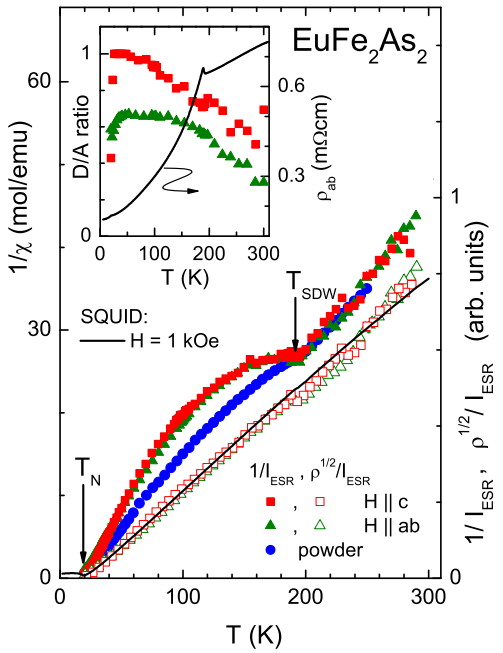

FIG. 2: (Color online) T-dependence of the inverse static susceptibility (left ordinate) of an $EuFe_2As_2$ single crystal measured with $H = 1000$ Oe aligned in the ab plane, the inverse ESR intensity $1/I_{\rm ESR}$ (right ordinate) for a single crystal and a powdered sample, and the skin-depth corrected values for the single crystal data. Inset: T-dependenc of the D/A-ratio and the in-plane resistivity of the single crystal.

i.e. a Lorentz line at resonance field $H_{\rm res}$ with half width at half maximum ΔH and a contribution $0 \leq \alpha \leq 1$ of dispersion to the absorption resulting in a characteristic asymmetry. This is typical for metals where the skin effect drives electric and magnetic components of the microwave field out of phase. The dispersion to absorption (D/A) ratio α depends on sample size, geometry, and skin depth. If the skin depth is small compared to the sample size, α approaches 1. As ΔH is of the same order of magnitude as $H_{\rm res}$, the counter resonance at $-H_{\rm res}$ was included in the fitting process as well [25].

The T-dependence of the inverse double-integrated signal intensity $I_{\rm ESR}$ is illustrated in Fig. 2 for both prominent orientations of the single crystal as well as for a powder sample. Below 50 K and above 200 K, the inverse intensity $1/I_{\rm ESR}$ follows a Curie-Weiss(CW)-like behavior with a CW temperature $\Theta \approx 19$ K in agreement with the static susceptibility. In the intermediate range one observes distinct deviations from linearity, which is related to the changes of the D/A ratio and the electrical resistivity shown in the inset of Fig. 2. The skin depth $\delta \propto \sqrt{\rho/\nu}$ and, hence, the partial volume of the sample probed by the microwave field decreases with decreasing temperature. These deviations are apparently reduced in the powder sample, because the microwave field penetrates nearly all sample volume due to the small grain size. After correction of the single-crystal data with respect to the skin depth, we recover the CW law in the entire temperature range (solid line in Fig. 2).

The T-dependences of $H_{\rm res}$ and ΔH are depicted in Fig. 3 for $H \parallel c$ and $H \parallel ab$ and compared to the corresponding data obtained in a powder sample. At high temperature the ESR spectra are approximately isotropic at a resonance field $H_{\rm res} \approx 3.41(3)$ kOe corresponding to a g value of 1.96(2), the linewidth increases linearly with temperature with a slope of approximately 8 Oe/K. Below $T_{\rm SDW}$ a pronounced anisotropy shows up in $H_{\rm res}$ and ΔH, which is illustrated in detail in the inset of Fig. 3. While a strong angular dependence with 180° periodicity appears, when rotating the field from the c axis into the ab plane, only a weak 90° modulation is observed, when rotating the field within the ab plane. The former can be ascribed to the dominant uniaxial crystal-electric field (CF) contribution, which will be determined below. The latter indicates the higher-order CF terms visible in the ab plane, which will not be further discussed here. On decreasing temperature the anisotropy first tends to a kind of saturation (see Fig. 4), but below 50 K it further diverges accompanied by a strong inhomogeneous broadening towards $T_{\rm N}$ due to the onset of magnetic fluctuations. In the following we will restrict the discussion to temperatures $T > T_{\rm N}$.

Metallic regime for $T > T_{\rm SDW}$: The ESR of local moments in metals is characterized by a shift of the g value $\Delta g = J(0)N(E_{\rm F})$ from its value in insulators and a linear increase of the linewidth $\Delta H \propto \langle J^2(q)\rangle N^2(E_{\rm F})T$ which both depend only on the conduction-electron density of

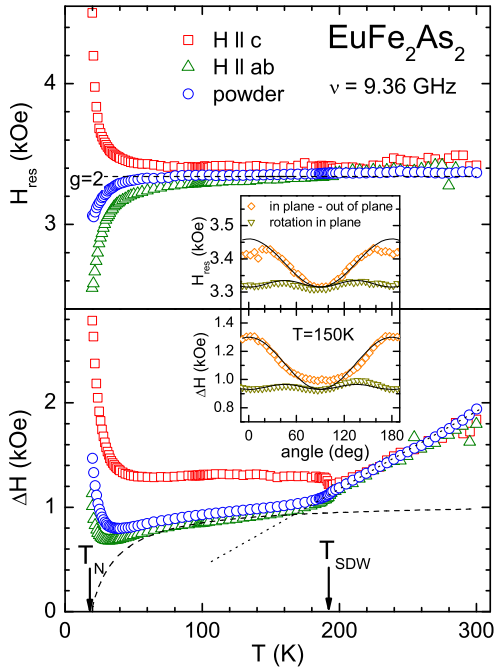

FIG. 3: (Color online) Temperature dependence of the resonance field $H_{\rm res}$ (upper frame) and linewidth ΔH (lower frame) of the ESR line in $EuFe_2As_2$ obtained for single crystal and powder sample. The insets illustrate the anisotropies of $H_{\rm res}$ and ΔH for rotation of the magnetic field within the ab plane as well as from the ab plane to the c direction. Solid lines $\propto \cos^2\theta$,$\sin^2\theta$ are to guide the eyes, the dotted line is linear fit, and the dashed line is a fit using Eq. 2.

states $N(E_{\rm F})$ at the Fermi energy $E_{\rm F}$ and the exchange constant J. The g shift results from the homogenous polarization of the CEs in the external field (Pauli susceptibility), thus J is taken at zero wave vector. The linewidth is determined by the spin-flip scattering of CEs at the local moments (Korringa relaxation) and, therefore, J is averaged over all possible scattering vectors q. Above $T_{\rm SDW}$ the observed increase of the linewidth by 8 Oe/K is a typical value for S-state $4f^7$ local moments in metals [24, 26, 27] and, therefore, is ascribed to a pure Korringa relaxation in a three-dimensional (3D) environment.

The negative g shift $\Delta g \approx -0.04$ is unusual, but its order of magnitude is typical for metals. The negative sign indicates peculiarities of the $4f$-$3d$ coupling which has been reported early in Gd doped Laves phases [27]. It is remarkable that inspite of the tetragonal symmetry of the crystal structure of $EuFe_2As_2$ resonance field and linewidth are isotropic within experimental accuracy, i.e. the CEs completely screen the ligand fields at the Eu site.

SDW state for $T < T_{\rm SDW}$: Below $T_{\rm SDW}$ the Korringa relaxation immediately disappears, although the resistivity even decreases more strongly with decreasing temperature. Concomitantly, the shift of the g value due to the polarization of the CEs diminishes and the averaged g

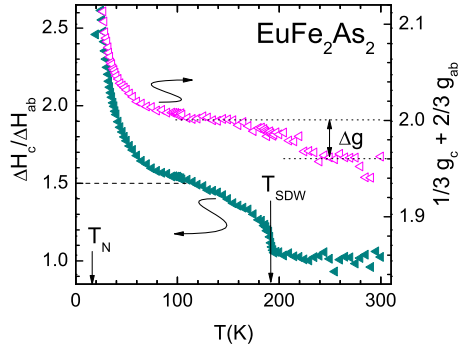

FIG. 4: (Color online) Temperature dependence of the relative anisotropy of the resonance linewidth $\Delta H_c/\Delta H_{ab}$ (left ordinate, closed symbols) and the averaged g value (open symbols, right ordinate) of an $EuFe_2As_2$ single crystal.

value $g = g_c/3 + 2g_{ab}/3$ below $T_{\rm SDW}$ corresponds to the typical value $g = 2.0$ for Eu^{2+} in an insulating system. This is a first indication that the formation of the SDW leads to a spatial confinement of the CEs to the FeAs layers. Moreover, a pronounced anisotropy shows up in the SDW state which reflects the symmetry of the ligand fields. In this temperature regime, if not too close to $T_{\rm N}$, the T-dependence of the linewidth can be well described in terms of Eu spin-spin relaxation typical for magnetic insulators. As pointed out by Huber *et al.*, in exchange coupled spin systems the linewidth

$$\Delta H(T) = \frac{\chi_0}{\chi(T)} \Delta H_\infty \qquad (2)$$

is determined by the ratio of single-ion susceptibility $\chi_0 \propto 1/T$ and the experimental susceptibility $\chi(T)$ of interacting spins multiplied by the high-temperature limit of the linewidth ΔH_∞ [28, 29]. This high temperature limit can be estimated following the theory of exchange narrowing of Anderson and Weiss [30] as

$$\Delta H_\infty = \frac{h}{g\mu_{\rm B}} \frac{\langle \nu_{\rm an}^2 \rangle}{\nu_{\rm ex}} \qquad (3)$$

where $\langle \nu_{\rm an}^2 \rangle$ denotes the second moment of the resonance-frequency distribution due to any anisotropic interaction like dipolar, hyperfine or crystal-electric field and $\nu_{\rm ex}$ is the exchange frequency between the Eu spins.

The dipolar contribution to the second moment reads

$$\langle \nu_{\rm DD}^2 \rangle = g^4 \mu_{\rm B}^4 \frac{3S(S+1)}{2h^2} \sum_{j \neq i} \frac{1 + \cos^2 \Theta_{ij}}{r_{ij}^6} \qquad (4)$$

where r_{ij} and Θ_{ij} denote the distance between spin i and j and the polar angle of the external magnetic field with respect to the direction of r_{ij} [31]. The main contribution results from the four nearest Eu neighbors at $r_{ij} = a = 3.907$ Å[12]. With $g = 2$ and $S = 7/2$ one obtains

$$\langle \nu_{\rm DD}^2 \rangle(\Theta) = 36\,{\rm GHz}^2 (2 + \sin^2 \Theta). \qquad (5)$$

Here the polar angle Θ is measured between the direction of the external field and the crystallographic c axis. The exchange constant J between the Eu^{2+} ions is determined from the CW temperature $\Theta_{CW} = 19\,K$ using the Weiss molecular field equations $3k_B\Theta_{CW} = JzS(S+1)$ with $z = 4$ exchange coupled nearest neighbors in the ab plane as $J/k_B \approx 0.9\,K$. Then the exchange frequency can be approximately estimated by $(h\nu_{ex})^2 \approx zS(S+1)J^2$ resulting in $\nu_{ex} \approx 150\,GHz$. Thus the linewidth due to dipolar broadening is determined as $\Delta H_\infty \approx 0.085\,kOe\ (2+\sin^2\Theta)$. This explains about 25% of the experimental linewidth, but exhibits an opposite anisotropy in comparison with the experimental data. The hyperfine interaction in ^{151}Eu ($^{151}A = 103\,MHz$) and ^{153}Eu ($^{153}A = 46\,MHz$) [31] is at least one order of magnitude smaller than the dipolar interaction, and hence can be neglected for the line broadening. Therefore, only the tetragonal CF can account for the observed anisotropy and magnitude of the linewidth.

The second moment of the leading uniaxial term of the CF is given by

$$\langle\nu^2_{CF}\rangle(\Theta) = \frac{4S(S+1)-3}{10}D^2(1+\cos^2\Theta) \qquad (6)$$

with the polar angle Θ measured between external field and crystallographic c axis [29]. This provides the proper anisotropy. The uniaxial zero-field splitting parameter D can be estimated from the experimentally observed asymptotic anisotropy of the linewidth at intermediate temperatures (dashed line in Fig. 4)

$$\frac{\Delta H_c}{\Delta H_{ab}} = \frac{\langle\nu^2_{CF}\rangle(0^\circ)+\langle\nu^2_{DD}\rangle(0^\circ)}{\langle\nu^2_{CF}\rangle(90^\circ)+\langle\nu^2_{DD}\rangle(90^\circ)} \approx 1.5. \qquad (7)$$

where $\langle\nu^2_{an}\rangle = \langle\nu^2_{DD}\rangle + \langle\nu^2_{CF}\rangle$ was assumed. Inserting Eqs. 5 and 6 yields $D \approx 5.5\,GHz$, which represents a reasonable order of magnitude [32]. With the obtained estimates for dipolar interaction, CF parameter and exchange frequency one obtains $\Delta H_\infty(0^\circ) \approx 1.1\,kOe$ in good agreement experiment.

In summary, the ESR properties in $EuFe_2As_2$ show distinct differences between the high-temperature phase and the SDW state below 190 K. Although the system remains metallic for all temperatures, the ESR linewidth and g value of the Eu^{2+} ions change from a typical behavior in a metallic environment with, e.g., a pure Korringa relaxation to characteristic anisotropic features as usually observed in insulators (e.g. spin-spin relaxation via dipolar and crystal fields). We ascribe this abrupt change to a local reduction of the 3D spin scattering due to a reduced concentration of CEs at the Eu site and their spatial confinement to the 2D FeAs layers in the SDW state.

Note. While finalizing this paper we became aware of an ESR study of Co doped $EuFe_2As_2$ for temperatures above 110 K, which shows a Korringa relaxation in agreement with our measurements [33].

We thank Anna Pimenov for the SQUID measurements. We acknowledge partial support by the Deutsche Forschungsgemeinschaft (DFG) via the Collaborative Research Center SFB 484 (Augsburg). The work at SNU was supported by NRL (Grant No. M10600000238) program.

* Electronic address: joachim.deisenhofer@physik.uni-augsburg.de

[1] Y. Kamihara *et al.*, J. Am. Chem. Soc. **130**, 3296 (2008).
[2] X. H. Chen et al., Nature **453**, 761(2008).
[3] M. Rotter *et al.*, Phys. Rev. Lett. **101**, 107006 (2008).
[4] H. S. Jeevan *et al.*, Phys. Rev. B **78**, 092406 (2008).
[5] F.-C. Hsu *et al.*, Proceedings of the National Academy of Sciences USA **105**, 14263 (2008).
[6] Y. Mizuguchi *et al.*, Appl. Phys. Lett. **93**, 152505 (2008).
[7] S. Medvedev *et al.*, Nature Mater. **8**, 630 (2009)
[8] J. Dong et al., Europhys. Lett. **83**, 27 006 (2008).
[9] M. Rotter *et al.*, Phys. Rev. B **78** 020503(R) (2008).
[10] M. Rotter *et al.*, New J. Phys. **11**, 025014 (2009).
[11] H. Raffius *et al.*, J. Phys. Chem. Solids **54**, 135 .
[12] H. S. Jeevan *et al.*, Phys. Rev. B **78**, 052502 (2008).
[13] D. Wu *et al.*, Phys. Rev. B **79**, 155103 (2009).
[14] Z. Ren et al., Phys. Rev. Lett. **102**, 137002 (2009).
[15] C. F. Miclea *et al.*, Phys. Rev. B **79**, 212509 (2009)
[16] T. Terashima *et al.*, J. Phys. Soc. Jap. **78**, 083701 (2009).
[17] A.S. Sefat *et al.*, Phys. Rev. Lett. **101**, 117004 (2008).
[18] A. Leithe-Jasper *et al.*, Phys. Rev. Lett. **101**, 207004 (2008).
[19] Q. J. Zheng *et al.*, arXiv:0907.5547 (2009).
[20] S. Jiang *et al.*, New J. Phys. **11**, 025007 (2009).
[21] M. Pfisterer and G. Nagorsen, Z. Naturforsch. **38b**, 811 (1983).
[22] B. Elschner and A. Loidl: in: *Handbook on the Physics and Chemistry of Rare Earth*, ed. by K. A. Gschneidner (Jr.), L. Eyring, and M.B. Maple, Elsevier Science B. V., Amsterdam, Vol. **30**, 375 (2000).
[23] Z. Ren *et al.*, Phys. Rev. B **78**, 052501 (2008).
[24] S. E. Barnes, Adv. Phys. **30**, 801 (1981).
[25] J.P. Joshi and S.V. Bhat, J. Mag. Res. **168**, 284 (2004).
[26] R.H. Taylor, Adv. Phys. **24**, 681 (1975).
[27] B. Elschner and A. Loidl: in: *Handbook on the Physics and Chemistry of Rare Earth*, ed. by K. A. Gschneidner (Jr.), L. Eyring, Elsevier Science B. V., Amsterdam, Vol. **24**, 221 (1997).
[28] R. Kubo and K. Tomita, J. Phys. Soc. Jpn. **9**, 888 (1954).
[29] D. L. Huber *et al.*, Phys. Rev. B **60**, 12155 (1999).
[30] P. W. Anderson and P. R. Weiss, Rev. Mod. Phys. **25**, 269 (1953).
[31] A. Abragam and B. Bleaney, *Electron Paramagnetic Resonance of Transition Ions*, Clarendon Press, Oxford (1970).
[32] H.-A. Krug von Nidda *et al.*, Phys. Rev. B **57**, 14344 (1998).
[33] J. J. Ying *et al.*, arXiv:0908.0037 (2009).